Geophysical Research Letters

RESEARCH LETTER
10.1029/2020GL088005

Turbidity Hysteresis in an Estuary and Tidal River Following an Extreme Discharge Event

David K. Ralston[1], Brian Yellen[2], Jonathan D. Woodruff[2], and Sarah Fernald[3]

[1]Woods Hole Oceanographic Institution, Woods Hole, MA, USA, [2]Department of Geosciences, University of Massachusetts, Amherst, MA, USA, [3]New York State Department of Environmental Conservation, Hudson, NY, USA

Key Points:
- Turbidity-discharge relationships are found in long-term observations (≥12 years) at multiple locations along the tidal Hudson River
- In the tidal freshwater, turbidity for a given discharge increased for 2 years following major discharge events and sediment input in 2011
- In the saline estuary, turbidity hysteresis was less apparent, consistent with greater background sediment concentrations and availability

Supporting Information:
- Figure S1

Correspondence to:
D. K. Ralston,
dralston@whoi.edu

Citation:
Ralston, D. K., Yellen, B., Woodruff, J. D., & Fernald, S. (2020). Turbidity hysteresis in an estuary and tidal river following an extreme discharge event. *Geophysical Research Letters*, *46*, e2020GL088005. https://doi.org/10.1029/2020GL088005

Received 17 MAR 2020
Accepted 24 JUN 2020
Accepted article online 17 JUL 2020

Abstract Nonlinear turbidity-discharge relationships are explored in the context of sediment sourcing and event-driven hysteresis using long-term (≥12-year) turbidity observations from the tidal freshwater and saline estuary of the Hudson River. At four locations spanning 175 km, turbidity generally increased with discharge but did not follow a constant log-log dependence, in part due to event-driven adjustments in sediment availability. Following major sediment inputs from extreme precipitation and discharge events in 2011, turbidity in the tidal river increased by 20–50% for a given discharge. The coherent shifts in the turbidity-discharge relationship along the tidal river over the subsequent 2 years suggest that the 2011 events increased sediment availability for resuspension. In the saline estuary, changes in the sediment-discharge relationship were less apparent after the high discharge events, indicating that greater background turbidity due to internal sources make event-driven inputs less important in the saline estuary at interannual time scales.

Plain Language Summary Turbidity is a widely accepted proxy for suspended sediment concentration and an important factor for contaminant transport and water quality. Here we show that turbidity depends on river discharge in long-term observations at multiple locations in an estuary. Such relationships are often used in rivers, but have not been commonly used in estuaries and tidal rivers, where tides and salinity also contribute to variability. Turbidity in the freshwater tidal region was more sensitive to discharge than in the saline estuary. Massive inputs of sediment due to extreme precipitation and flooding in 2011 resulted in increased sediment availability in the tidal river over multiple years. Turbidity throughout the tidal river was elevated for 2 years following the events, but changes were not apparent in the saline estuary. The observations provide guidance on recovery time scales for estuaries and tidal rivers to event-driven sediment inputs, which affects the delivery of material from the watershed to the coastal ocean as well as other impacts on water clarity.

1. Introduction

Due to the challenges in continuously monitoring suspended sediment concentration (SSC), SSC and sediment discharge in rivers are often empirically related to volumetric freshwater discharge (Helsel & Hirsch, 2002). Volumetric discharge varies by orders of magnitude at event and seasonal time scales, and it is the dominant factor controlling variability in sediment discharge. Sediment discharge increases nonlinearly with volumetric discharge, commonly increasing to approximately the cube of river discharge at high flow (Nash, 1994; Syvitski et al., 2000). Consequently, large, relatively infrequent events disproportionately contribute to cumulative sediment discharges.

Sediment-discharge rating curves are often treated as static, and yet variability in precipitation patterns, vegetation, land use, and tectonic activity can all affect sediment delivery and sediment-discharge relationships (Morehead et al., 2003; Walling, 1977; Warrick & Rubin, 2007; Yellen et al., 2016). Disturbance from extreme floods can increase sediment concentrations for months to years as rivers adjust to bed incision and landslide scarps revegetate (Ahn et al., 2017; Dethier et al., 2016; Gray, 2018; Warrick et al., 2013). The duration and timing of low-discharge conditions can affect in-stream storage and SSC during subsequent higher discharge periods (Gray et al., 2014; Walling et al., 1998). Sampling frequency can also contribute to uncertainty or introduce bias into sediment discharge measurements (Coynel et al., 2004), and the variability in time scales of watershed response that can be diagnosed depends on the functional form of the sediment-discharge relation (Ahn & Steinschneider, 2019).

Rivers supply sediment to coastal regions, where tides, waves, and density-driven circulation also play central roles in sediment transport. In estuaries, salinity gradients drive landward near-bottom circulation that leads to sediment trapping and regions of higher sediment concentration, or estuarine turbidity maxima (ETMs) (Burchard et al., 2018; Postma, 1961). River discharge alters sediment input from the watershed but also affects the salinity distribution and thus the location and magnitude of sediment trapping at seasonal and event time scales. Tidal currents also contribute to variability in SSC, directly through sediment resuspension and indirectly by affecting the salinity distribution. In the tidal freshwater part of an estuary, tidal resuspension and sediment supply from the river are the key factors in SSC variability (Dalrymple & Choi, 2007; Ralston & Geyer, 2017). Tidal freshwater regions provide crucial links in the movement of material to the coastal ocean, and yet they have received less study than fluvial or estuarine environments (Hoitink & Jay, 2016).

This study uses long-term (≥12-year) observations to characterize turbidity-discharge relationships in a tidal river and estuary, including the response following sediment inputs from major discharge events. Because it is easier to measure, turbidity is often used as a proxy for SSC (Ahn et al., 2017; Yellen et al., 2014), and turbidity has been shown to correlate well with SSC in the tidal river (Ralston & Geyer, 2017) and within the watershed of the study (McHale & Siemion, 2014). In late summer 2011, tropical cyclones Irene and Lee delivered intense precipitation over much of the U.S. Northeast, increasing discharge and sediment delivery. In the Delaware estuary, sediment input of 1.4 Mt in 2 weeks was similar to the long-term annual average, and SSC in the ETM of the Delaware remained elevated for several months (Sommerfield et al., 2017). In the Connecticut River estuary, input from Irene of 1.2 Mt was twice the annual average, and the sediment-discharge relationship in the tidal river was elevated for the following 2 years compared to before the storm (Yellen et al., 2014). In the Hudson River estuary, sediment input from Irene and Lee was about 2.7 Mt, more than twice the annual average (Ralston et al., 2013; Wall et al., 2008). The events increased turbidity in the months following the events, but the response to this sediment input has not been examined at longer time scales. In this study, we use long-term monitoring data to assess the turbidity-discharge relationships at multiple locations along the tidal Hudson River and quantify the time scales over which the discharge events altered turbidity in the system.

2. Methods

2.1. Site Description

The Hudson River estuary extends about 265 km from the Atlantic Ocean to tidal limit at Troy (NY). Along-estuary distances in the Hudson are typically reported with respect to The Battery in New York Harbor as 0 river km (rkm), but The Battery is located about 25 km landward of the natural mouth between Sandy Hook and Rockaway Peninsula. The tidal range averages about 1.5 m at the mouth, decreases to 1 m midestuary, and increases to 1.5 m at the head of tides (Ralston et al., 2019). The salinity intrusion varies from about 40 rkm during high river discharge to 120 rkm during low discharge (Bowen & Geyer, 2003; Ralston et al., 2008).

The primary ETM in the Hudson is located near 20 rkm, formed by bottom salinity fronts associated with a constriction (Geyer et al., 2001; Traykovski et al., 2004). During moderate and low discharge, a secondary ETM forms near 55 rkm (Nitsche et al., 2010; Ralston et al., 2012). In the primary ETM, near-bottom sediment concentrations can exceed 1 g L^{-1}, and concentrations are greater than 100 mg L^{-1} in much of the saline estuary. In the tidal river, sediment concentrations are generally less than 100 mg L^{-1} and vary with river discharge and tidal forcing (Ralston & Geyer, 2017; Wall et al., 2008). Sediment inputs come from the two largest tributaries, the Mohawk and Upper Hudson Rivers, which converge just above the tidal limit. Numerous smaller tributaries also discharge into the tidal Hudson, cumulatively increasing the sediment load by 30–70% (Wall et al., 2008).

2.2. Observations

Turbidity data were collected from monitoring stations located along the estuary. Data were accessed through the Hudson River Environmental Conditions Observing System (www.hrecos.org), which organizes monitoring data from multiple partner organizations, and the Centralized Data Management Office (cdmo.baruch.sc.edu). Monitoring stations were at Schodack Island (212 rkm, available 2008–2019, partner

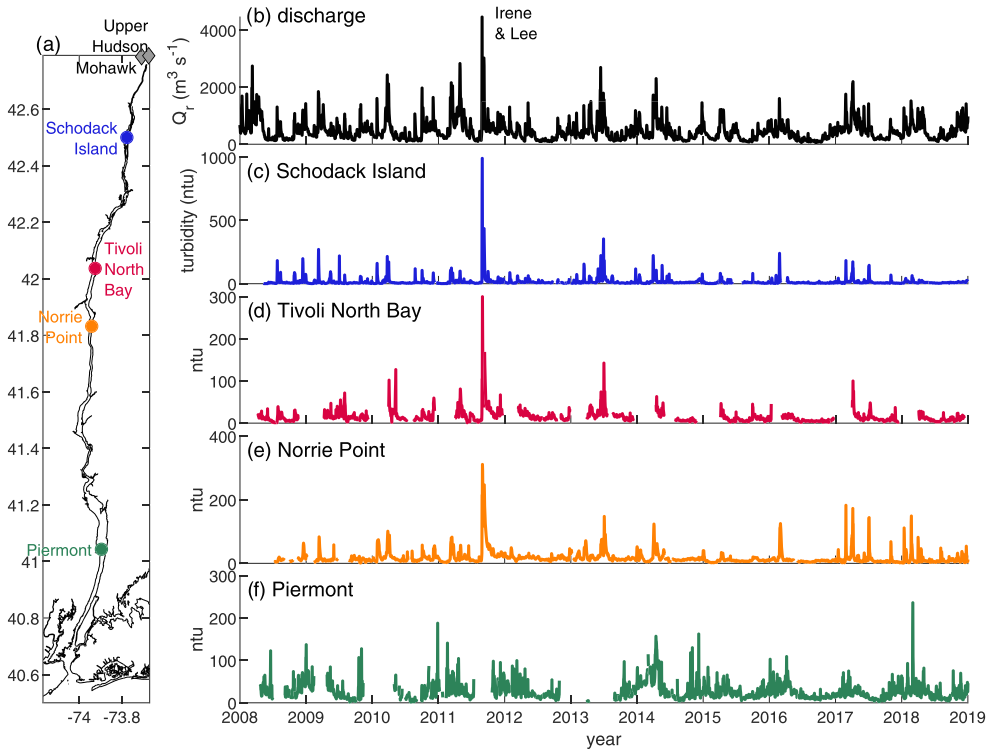

Figure 1. Turbidity at monitoring stations along the estuary. (a) Station locations, (b) daily average discharge from the Upper Hudson and Mohawk, noting tropical storms Irene and Lee in 2011, and (c–f) daily median turbidity from Schodack Island, Tivoli North Bay, Norrie Point, and Piermont.

organization Cary Institute of Ecosystem Studies), Tivoli North Bay (156 rkm, 2000–2019, Hudson River National Estuarine Research Reserve, HRNERR), Norrie Point (132 rkm, 2008–2019, HRNERR), and Piermont (37 rkm, 2008–2019, Lamont-Doherty Earth Observatory) (Figure 1). Under most forcing conditions, Piermont is in the saline estuary and the other three stations are in the tidal freshwater (Hoitink & Jay, 2016).

All stations recorded near-surface turbidity. Time series were processed for quality control based on visual inspection to remove spurious outliers or anomalous trends indicative of instrument fouling. The quality control removed 0.3% to 2.8% of the measurements, depending on the station. The Tivoli North Bay sensor is located in a small channel connecting to a side embayment, so we only used measurements during flood tides. Daily median turbidity values were used to minimize the influence of individual bad measurements on longer term variability. At Tivoli, water samples were collected, filtered, dried, and weighed to measure suspended solids concentration for comparison with turbidity. The regression slope for total suspended solids (mg L^{-1}) was 1.2 times the turbidity (NTU, $r^2 = 0.52$, $n = 219$). Turbidity sensors at the other stations were not calibrated to SSC, but previous studies in the saline estuary and tidal river have also found calibrations with slopes of around 1 (Ralston & Geyer, 2017; Ralston et al., 2013).

Volumetric discharge (Q_r) and sediment discharge (Q_s) measurements were collected from U.S. Geological Survey (USGS) gauging stations on the Mohawk and Upper Hudson. The Mohawk (at Cohoes, 01357500) has volumetric discharge 1917–2019 and sediment discharge 1954–1959, 1976–1979, and 2002–2019. The Upper Hudson (Waterford, 01335770) has volumetric discharge 1887–1956 and 1976–2019 and sediment discharge 1976–2014. Mean daily mean SSC were calculated with $SSC = Q_s/Q_r$.

Turbidity was related to Q_r by locally weighted scattered smoothing, or LOWESS (Cleveland, 1979; Helsel & Hirsch, 2002). The LOWESS approach has been used for sediment discharge rating curves in rivers, including in trend analyses following discharge events (Gray, 2018; Warrick et al., 2013). LOWESS regressions were calculated for log-transformed discharge and turbidity with a smoothing factor of 0.25. A bias

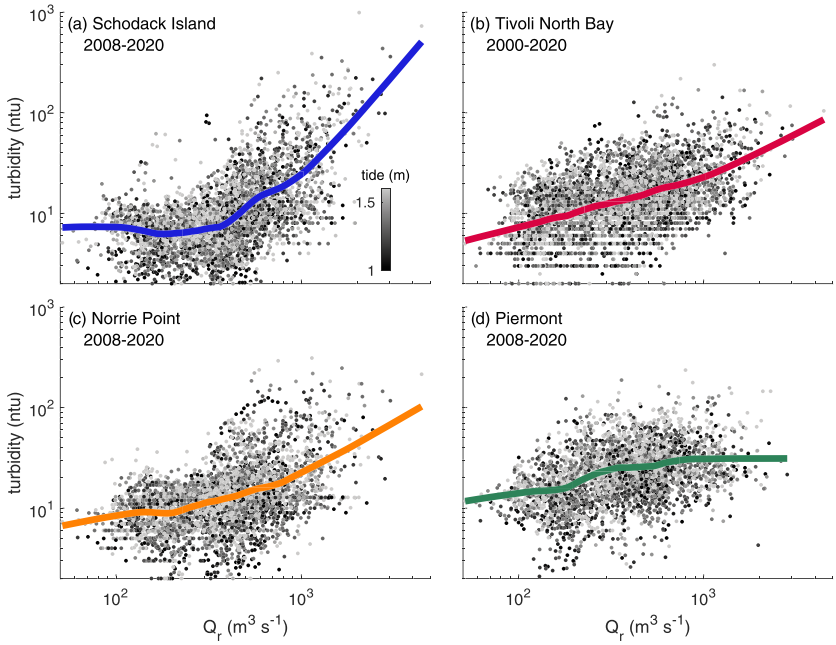

Figure 2. Turbidity versus river discharge (Q_r) at (a) Schodack Island, (b) Tivoli North Bay, (c) Norrie Point, and (d) Piermont. Daily turbidity data are in black, and LOWESS regressions are colored. Marker shading represents tidal amplitude based on the water level at The Battery (NOAA # 8518750).

correction factor was included to calculate turbidity from discharge using the regression (Cohn, 1995; Ferguson, 1986), with the form $C = 10\text{^}(C_{out} + \sigma^2/2)$, where C_{out} is the output from the LOWESS regression to $\log_{10}(Q_r)$ and σ^2 is the variance of the residual. The variance of the residual was calculated in fractional subsets of Q_r similar to the LOWESS smoothing factor to account for variability in the regression fit.

3. Results

Over the observation period (2008–2019), Irene and Lee accounted for the highest river discharge and observed turbidity (Figure 1). The turbidity during and immediately following the 2011 events was greatest in the upper tidal river at Schodack Island, with 1,000 NTU during Irene and 500 NTU during Lee. At the Tivoli North Bay and Norrie Point stations in the tidal river, turbidity was 200–300 NTU during the events. Increased turbidity was recorded during other high discharge periods, including spring freshets in 2013, 2014, and 2016, but those maxima were less than half than during Irene. In the saline estuary, the Piermont station was not operational during the 2011 events. During other years, the maximum turbidity at Piermont was typically around 100 NTU, with generally higher turbidity during the winter and spring and lower in the summer.

Turbidity from the four stations is plotted against discharge, and all the locations have positive slopes (Figure 2). At Schodack Island, the turbidity dependence on discharge has a form similar to many rivers (Nash, 1994), with a greater slope at higher discharge ($Q_r > 400$ m^3 s^{-1}) and weaker dependence at lower Q_r. Schodack is in a shallow and sandy part of the tidal river (Collins & Miller, 2012; Nitsche et al., 2007), so resuspension of fine sediment is limited and turbidity varies strongly with river inputs. The slightly negative slope at low discharge may be an artifact of limited data or may be due to increased organic particles during summer low discharge (Ralston & Geyer, 2017). Farther seaward, at the Tivoli and Norrie Point stations, turbidity increases more gradually with discharge (Figures 2b and 2c). Discharge varies annually by about an order of magnitude, and turbidity in the tidal river varies by more than an order of magnitude. The turbidity variability in the tidal freshwater river is greater than that in the saline estuary, where the annual range typically spans a factor of 2–3 (Bokuniewicz & Arnold, 1984; Ralston & Geyer, 2017; Ralston et al., 2012). Correspondingly, the turbidity-discharge regression at Piermont has a narrower range than

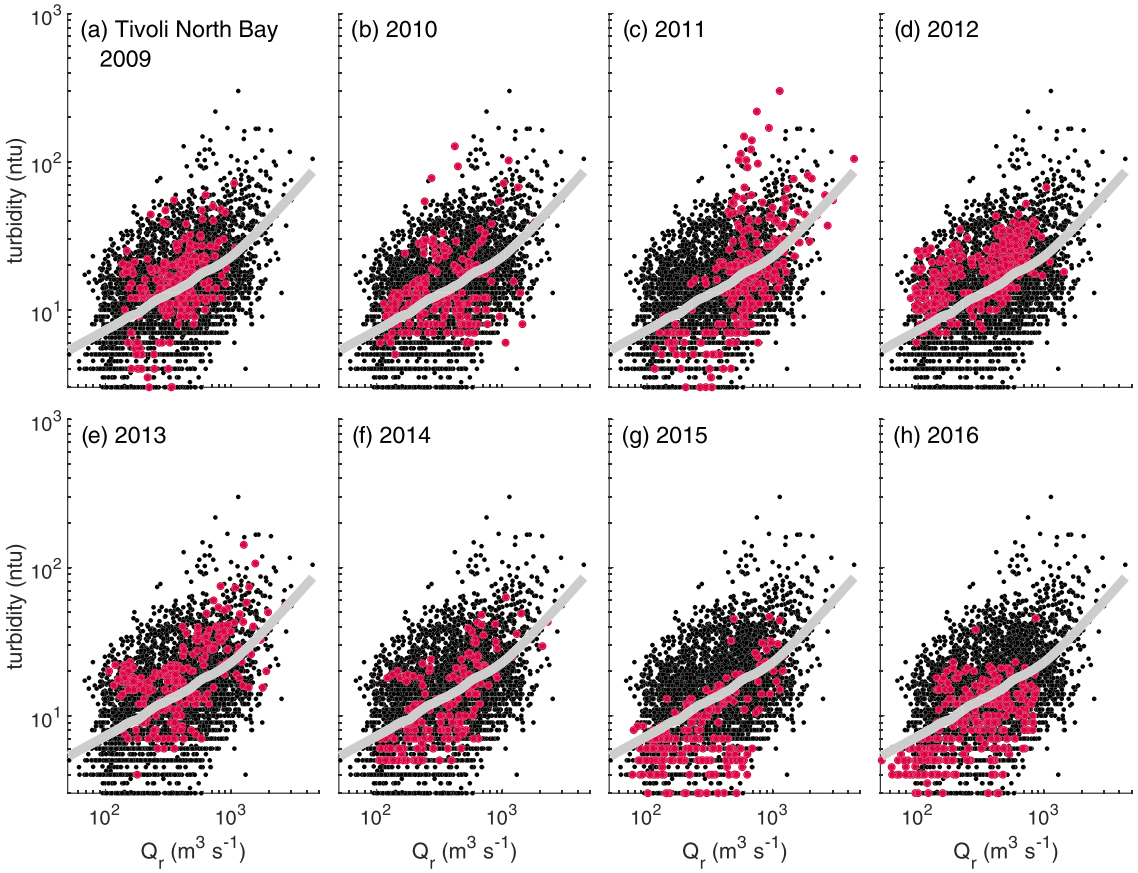

Figure 3. (a–h) Turbidity versus river discharge at Tivoli North Bay by water year from 2009 to 2016. The full record is in black, and data for each year are colored. The LOWESS fit to the full record is gray.

those at the tidal river stations, and discharge dependence is weaker (Figure 2d). The LOWESS fits between discharge and turbidity at the tidal river stations had higher correlations (r^2 = 0.42 at Schodack, 0.24 at Tivoli, and 0.19 at Norrie) than at Piermont in the saline estuary (r^2 = 0.12).

Scatter in the turbidity-discharge relationships is due to the many processes that affect turbidity in addition to discharge. Tidal amplitude affects sediment resuspension, and residuals in the LOWESS fits were positively correlated with tidal amplitude at all four locations, but the correlations were weak ($r^2 < 0.005$ at the tidal river stations and $r^2 = 0.02$ at the estuarine Piermont station). Sediment resuspension and trapping can also vary with the salinity distribution, wind, and bed sediment properties. Lags in sediment transport can be weeks to months (Ralston & Geyer, 2009, 2017), distorting the correspondence between the daily discharge and turbidity along the estuary. Antecedent discharge conditions affect sediment availability in the estuary, with fine sediment accumulating during higher discharge and subsequently increasing tidal resuspension, potentially changing the relationship with daily discharge (Wall et al., 2008).

To evaluate whether inputs from Irene and Lee affected sediment availability in the estuary and thus turbidity over longer time scales, the turbidity versus discharge relationship is considered on a yearly basis. Turbidity time series are segmented by water year (1 October to 30 September) to reflect the seasonality of higher discharge in the late fall, winter, and spring and lower discharge summer. As an example, observations for individual years are shown for Tivoli North Bay and compared to the regression for the entire record (Figure 3). Clustering of median daily observations above or below the LOWESS fit of the full 12-year record represents a shift in the turbidity-discharge relationship. Increased sediment availability following Irene and Lee corresponds to higher than average turbidity (for a given discharge) in 2012 and 2013, as well as a few anomalously high turbidity observations during water year 2011 (Figures 3d and 3e). In contrast, turbidity tends to be less than the long-term regression for most discharge conditions in 2015 (Figure 3g).

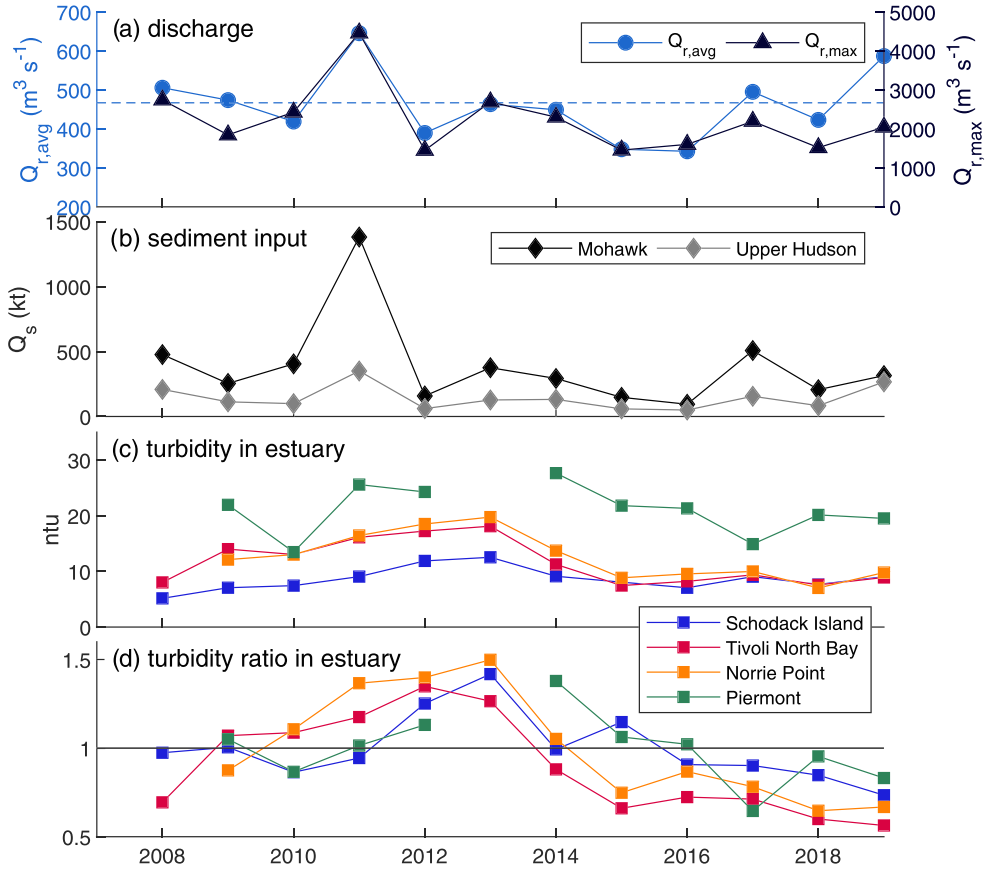

Figure 4. Discharge and turbidity by water year. (a) Mean and maximum discharge of the Upper Hudson and Mohawk rivers, (b) annual sediment input from the Mohawk and Upper Hudson, (c) annual average turbidity in the tidal river and estuary, and (d) annual average of the ratio of measured turbidity to that predicted by the long-term Q_r regressions (Figure 2).

Over the turbidity observation period, the combined annual average discharge from Upper Hudson and Mohawk Rivers varied by almost a factor of 2, from 350 to 650 m^3 s^{-1}, and the maximum combined daily discharge varied by about a factor of 3, from 1,460 to 4,460 m^3 s^{-1} (Figure 4a). Annual sediment inputs from the rivers were calculated based on observed discharge and regressions to long-term sediment discharge observations (Ralston et al., 2020), since the direct measurements of sediment discharge did not span the full period (Figure 4b). The most notable variability in sediment inputs over this period was the large increase from the Mohawk with the storm events in 2011.

Annual averages of turbidity in the tidal freshwater and saline estuary varied by about a factor of 2 over the same period (Figure 4c). The interannual variability in average turbidity is in part due to variation in river discharge, with higher turbidity during years with greater average discharge. However, the goal here is to assess whether hysteresis in the turbidity-discharge relationship may also contribute. To quantify this, we calculate the annual average of the ratio of the measured turbidity to that predicted by the turbidity-discharge regressions shown in Figure 2. This turbidity ratio represents the factor by which the turbidity differed from the long-term regression, accounting for interannual variations in discharge (Figure 4d). Discretization at semi-annual and quarter-annual intervals was also examined, with similar (but noisier) results.

Similar interannual variation in turbidity relative to the long-term regression was observed among the three tidal freshwater stations (i.e., Schodack, Tivoli, and Norrie Point), despite separation of about 80 km and differences in local bed sediment. In 2012 and 2013, turbidity at all three locations was greater than expected based on the long-term regression, by factors of about 1.4 at Schodack, 1.3 at Tivoli, and 1.5 at Norrie. In 2010 and prior years, the turbidity factors were close to or less than 1 at all three stations. The turbidity factor increased at Tivoli and Norrie Point in 2011, but this could be due to large sediment inputs from tributaries

near these stations during Irene and Lee at the end of 2011 water year (Ralston et al., 2013). After 2013, the turbidity ratios returned to values similar to 1, representing a return to long-term average conditions. Values less than 1 before and after 2011–2014 reflect that the long-term regression includes the elevated turbidity from Irene and Lee. Average turbidity in the tidal river thus depended both on Q_r that year and on hysteresis in the turbidity-discharge relationship. For example, the mean Q_r in 2012 (390 $m^3\ s^{-1}$) was less than average (460 $m^3\ s^{-1}$), and yet the average turbidity that year was the second highest overall (Figure 4c). In 2013, the turbidity increased in part because the discharge increased, but also because of the above-average turbidity-discharge relationship (Figure 4d).

Another approach to characterizing the temporal variability in the turbidity-discharge relationship is to calculate the slope of the cumulative residual between the observed and predicted turbidity (Gray, 2018). Periods when observed turbidity was greater than expected have a positive slope for the cumulative residual, and periods with turbidity less than expected have negative slopes. Results using the cumulative residual slopes were consistent with the turbidity ratios, with positive slopes during years with turbidity ratio greater than 1 and negative residuals for turbidity ratios less than 1 (Figure S1 in the supporting information). Similarly, the cumulative residual slopes at the tidal river stations were maximum in 2012 and 2013, after Irene and Lee, and decreased to zero or negative values in 2014 or 2015 and after.

The temporal variability in the turbidity-discharge relationship was coherent among the freshwater tidal stations, but observations in the saline estuary did not exhibit the same interannual response (Figure 4c). For example, the turbidity ratio at Tivoli was strongly correlated with that at Norrie Point ($r^2 = 0.93$, $p < 0.001$, $n = 11$) and had a weaker correlation with Schodack Island ($r^2 = 0.63$, $p = 0.028$, $n = 12$), but the correlation with Piermont in the saline estuary was not significant ($r^2 = 0.33$, $p = 0.35$, $n = 10$). The Piermont station exhibited only a modest increase in the turbidity ratio in 2012 after Irene and Lee (with a data gap in 2013) and in general has less variability in the turbidity-discharge relationship.

The turbidity ratios in the estuary were not significantly correlated with the year-to-year variability in the sediment mass inputs from the Mohawk and Upper Hudson (Figure 4b). To evaluate the influence of the variability in watershed inputs, we also calculated the residual of the LOWESS regressions of $\log_{10}(SSC)$ versus $\log_{10}(Q_r)$ for the tributaries on an annual basis. Precipitation from Irene and Lee was focused in the Mohawk watershed and the Catskill Mountains east of the Hudson, leading to mass wasting, increased erosion, and potential hysteresis in the sediment-discharge relationship for these regions (Ahn & Steinschneider, 2019). In water years 2012–2014 following the events, the average *SSC* in the Mohawk increased by a factor of about 1.2 above the regression values, but the Mohawk turbidity ratio was not significantly correlated with the turbidity ratios in the estuary. As expected from precipitation patterns during Irene-Lee, the turbidity-discharge ratio for the Upper Hudson did not change post-event.

4. Summary and Discussion

Long-term monitoring data allow for characterization of turbidity-discharge relationships in the estuary that might be obscured by variability at tidal to seasonal time scales. In the tidal freshwater, turbidity depended strongly on discharge (Figure 2). Average residuals between observed turbidity and that predicted from the discharge regressions were coherent among stations in the tidal river, with increased turbidity in the 2 years following tropical storms Irene and Lee (Figure 4). Similarly, in New England watersheds, adjustment time scales for channel morphology following Irene, and for subsequent, smaller discharge events, were found to be 1–2 years (Renshaw et al., 2019). Watershed sediment supply depends in part on revegetation of landslides and bank failures, which adjusts at multiyear time scales (Dethier et al., 2016; Gray et al., 2014; Yellen et al., 2014). Watershed sediment supply from the Mohawk increased relative to discharge during 2012–2014 due to these geomorphic adjustments in its steep tributaries (Ahn & Steinschneider, 2019) and thus may contribute to the 2012–2013 increase in the turbidity factor in the tidal river (Figure 4d). However, we observed a similar increase in the SSC factor relative to the discharge relation for the Mohawk in 2017, when the turbidity factors at tidal river stations were less than or equal to 1. Therefore, the increased turbidity in the tidal river was at least in part determined by the pulsed input to the mobile pool, the signal of which relaxed over 2013–2014 (Figure 4d). The similar response among stations separated by 80 km suggests that the increased sediment availability was not limited to a small region or due to localized influence of a particular tributary.

Increased turbidity suggests an increase in SSC, particularly for a fixed particle size distribution. Alternatively, temporal decreases in the dominant particle size could increase turbidity and change the relationship to SSC (Downing, 2006). Seasonal variation in the slope between turbidity and SSC of about a factor of 2 has been noted in the tidal Hudson, likely due to changes in particle size with discharge (Ralston & Geyer, 2017). Thus, the shift toward higher turbidity ratios may reflect a combination of greater availability and finer grain size following discharge events (Yellen et al., 2016). The contribution of organic material to turbidity also varies seasonally, as on average SPM samples in summer and fall had higher organic fractions than in the first half of the year. However, our averaging of turbidity ratios at annual time scales reduces effects of seasonal variation in the relationship between turbidity and SPM on discharge dependence. Due to the relatively turbid conditions and low light availability in the Hudson, phytoplankton are also not expected to contribute significantly to the turbidity signal (Cole et al., 1992).

The turbidity responses differed between the tidal river and saline estuary, where changes in the turbidity-discharge relationship were less apparent following the discharge events. In the tidal river, SSC tends to be lower and the bed less muddy than in the saline estuary (Nitsche et al., 2007). The sediment available for resuspension at event to seasonal time scales has been termed the mobile sediment pool (Geyer & Ralston, 2018; Schoellhamer, 2011; Wellershaus, 1981). While the size of the mobile pool is difficult to quantify, the persistent increase in turbidity in the tidal river following Irene and Lee suggests that the sediment input from the storms represented a major increase in the size of the mobile pool. Based on sediment fluxes measured in the lower tidal river, about two thirds of the sediment input by the events remained in the tidal river several months after the events (Ralston et al., 2013), and the 2-year period of increased turbidity may be indicative of the time scale for the tidal river to adjust back to pre-storm conditions.

In the saline estuary, turbidity on average is greater, the bed is muddier, and the mobile pool is larger than in the tidal river. Previous studies have highlighted the seasonal to annual variation in SSC and deposition (Geyer et al., 2001; Woodruff et al., 2001). Observations in the lower ETM found that the freshets in 1998 and 1999 each deposited about 0.3 Mt of new sediment, despite large differences in the watershed sediment inputs in those years (Woodruff et al., 2001). The limited interannual variability in the turbidity-discharge residual at Piermont found here is consistent with this decoupling between deposition in the ETM and the watershed inputs. If the mobile pool in the saline estuary is many times the annual average input, then the fractional increase from Irene and Lee may be minor. Similarly, in San Francisco Bay, a decrease in sediment supply associated with dam construction did not affect sediment concentrations until decades later, first in the tidal freshwater Delta and subsequently in the saline estuary (Hestir et al., 2013; Schoellhamer, 2011; Schoellhamer et al., 2013). In the Penobscot estuary, the mobile sediment pool was estimated to be 6–8 times the annual average input based on recovery time scales following a contaminant release (Geyer & Ralston, 2018).

Differences between the tidal river and saline estuary in the hysteresis of the turbidity-discharge relationships reflect the relative coupling between sediment supply and river discharge. In the saline estuary, the mobile pool is large compared to the annual supply, such that a major discharge event does not drastically increase sediment availability. In contrast, fine-grained bed sediment in the tidal river is more limited, so event inputs represent a fractionally bigger change, and turbidity is increased for a couple of years as the added sediment gradually moves seaward and deposits in lower energy shoals and wetlands (Ralston & Geyer, 2017; Yellen et al., 2020). For comparison, the hysteresis in turbidity-discharge relationship in the tidal river is similar in duration to observations on steep streams following Irene (Renshaw et al., 2019) but shorter in duration than observed in rivers along the U.S. West Coast, where sediment concentrations remained elevated for 5 years or longer after events (Gray, 2018; Warrick et al., 2013). Long-term measurements at stream gauging stations allow for assessment of the variability in turbidity/sediment-discharge relationships in the watershed, but such long-term measurements are far less common in estuaries. These results point to the utility of such measurements for assessing the multiple time scales of sediment variability in other estuaries.

Data Availability Statement

The data used in this study were all downloaded from publicly available sources (USGS, https://waterdata.usgs.gov/nwis; HRECOS, https://hrecos.org/; or CDMO, http://cdmo.baruch.sc.edu/) as described in the Methods section. Data used in the figures are available at http://doi.org/10.5281/zenodo.3936047

Acknowledgments

This work was sponsored by the National Estuarine Research Reserve System Science Collaborative, funded by the National Oceanic and Atmospheric Administration and managed by the University of Michigan Water Center (NAI4NOS4190145), with additional support to Yellen and Woodruff from USGS Cooperative Agreement No. G19AC00091.

References

Ahn, K.-H., & Steinschneider, S. (2019). Time-varying, nonlinear suspended sediment rating curves to characterize trends in water quality: An application to the Upper Hudson and Mohawk Rivers, New York. *Hydrological Processes*, *33*, 1865–1882. https://doi.org/10.1002/hyp.13443

Ahn, K.-H., Yellen, B., & Steinschneider, S. (2017). Dynamic linear models to explore time-varying suspended sediment-discharge rating curves. *Water Resources Research*, *53*, 4802–4820. https://doi.org/10.1002/2017WR020381

Bokuniewicz, H. J., & Arnold, C. L. (1984). Characteristics of suspended sediment transport in the lower Hudson River. *Northeastern Environmental Science*, *3*, 184–189.

Bowen, M. M., & Geyer, W. R. (2003). Salt transport and the time-dependent salt balance of a partially stratified estuary. *Journal of Geophysical Research*, *108*(C5), 3158. https://doi.org/10.1029/2001JC001231

Burchard, H., Schuttelaars, H. M., & Ralston, D. K. (2018). Sediment trapping in estuaries. *Annual Review of Marine Science*, *10*(1), 371–395. https://doi.org/10.1146/annurev-marine-010816-060535

Cleveland, W. S. (1979). Robust locally weighted regression and smoothing scatterplots. *Journal of the American Statistical Association*, *74*(368), 829–836. https://doi.org/10.1080/01621459.1979.10481038

Cohn, T. A. (1995). Recent advances in statistical methods for the estimation of sediment and nutrient transport in rivers. *Reviews of Geophysics*, *33*(S2), 1117–1123. https://doi.org/10.1029/95RG00292

Cole, J. J., Caraco, N. F., & Peierls, B. L. (1992). Can phytoplankton maintain a positive carbon balance in a turbid, freshwater, tidal estuary? *Limnology and Oceanography*, *37*(8), 1608–1617. https://doi.org/10.4319/lo.1992.37.8.1608

Collins, M. J., & Miller, D. (2012). Upper Hudson River estuary (USA) floodplain change over the 20th century. *River Research and Applications*, *28*(8), 1246–1253. https://doi.org/10.1002/rra.1509

Coynel, A., Schäfer, J., Hurtrez, J.-E., Dumas, J., Etcheber, H., & Blanc, G. (2004). Sampling frequency and accuracy of SPM flux estimates in two contrasted drainage basins. *Science of the Total Environment*, *330*(1-3), 233–247. https://doi.org/10.1016/j.scitotenv.2004.04.003

Dalrymple, R. W., & Choi, K. (2007). Morphologic and facies trends through the fluvial-marine transition in tide-dominated depositional systems: A schematic framework for environmental and sequence-stratigraphic interpretation. *Earth-Science Reviews*, *81*(3-4), 135–174. https://doi.org/10.1016/j.earscirev.2006.10.002

Dethier, E., Magilligan, F. J., Renshaw, C. E., & Nislow, K. H. (2016). The role of chronic and episodic disturbances on channel-hillslope coupling: The persistence and legacy of extreme floods. *Earth Surface Processes and Landforms*, *41*(10), 1437–1447. https://doi.org/10.1002/esp.3958

Downing, J. (2006). Twenty-five years with OBS sensors: The good, the bad, and the ugly. *Continental Shelf Research*, *26*(17-18), 2299–2318. https://doi.org/10.1016/j.csr.2006.07.018

Ferguson, R. I. (1986). River loads underestimated by rating curves. *Water Resources Research*, *22*(1), 74–76. https://doi.org/10.1029/WR022i001p00074

Geyer, W. R., & Ralston, D. K. (2018). A mobile pool of contaminated sediment in the Penobscot estuary, Maine, USA. *Science of the Total Environment*, *612*, 694–707. https://doi.org/10.1016/j.scitotenv.2017.07.195

Geyer, W. R., Woodruff, J. D., & Traykovski, P. (2001). Sediment transport and trapping in the Hudson River estuary. *Estuaries*, *24*(5), 670–679. https://doi.org/10.2307/1352875

Gray, A. B. (2018). The impact of persistent dynamics on suspended sediment load estimation. *Geomorphology*, *322*, 132–147. https://doi.org/10.1016/j.geomorph.2018.09.001

Gray, A. B., Warrick, J. A., Pasternack, G. B., Watson, E. B., & Goñi, M. A. (2014). Suspended sediment behavior in a coastal dry-summer subtropical catchment: Effects of hydrologic preconditions. *Geomorphology*, *214*, 485–501. https://doi.org/10.1016/j.geomorph.2014.03.009

Helsel, D. R., & Hirsch, R. M. (2002). *Statistical methods in water resources* (Vol. 323). Reston, VA: U.S. Geological Survey.

Hestir, E. L., Schoellhamer, D. H., Morgan-King, T., & Ustin, S. L. (2013). A step decrease in sediment concentration in a highly modified tidal river delta following the 1983 El Niño floods. *Marine Geology*, *345*. A multi-discipline approach for understanding sediment transport and geomorphic evolution in an estuarine-coastal system: San Francisco Bay, 304–313. https://doi.org/10.1016/j.margeo.2013.05.008

Hoitink, A. J. F., & Jay, D. A. (2016). Tidal river dynamics: Implications for deltas. *Reviews of Geophysics*, *54*, 240–272. https://doi.org/10.1002/2015RG000507

McHale, M. R., & Siemion, J. (2014). *Turbidity and suspended sediment in the upper Esopus Creek watershed, Ulster County, New York* (Scientific Investigations Report 2014–5200, pp. 1–42). Troy, NY: U.S. Geological Survey. https://doi.org/10.3133/sir20145200

Morehead, M. D., Syvitski, J. P., Hutton, E. W. H., & Peckham, S. D. (2003). Modeling the temporal variability in the flux of sediment from ungauged river basins. *Global and Planetary Change*, *39*(1-2), 95–110. https://doi.org/10.1016/S0921-8181(03)00019-5

Nash, D. B. (1994). Effective sediment-transporting discharge from magnitude-frequency analysis. *Journal of Geology*, *102*(1), 79–95. https://doi.org/10.1086/629649

Nitsche, F. O., Kenna, T. C., & Haberman, M. (2010). Quantifying 20th century deposition in complex estuarine environment: An example from the Hudson River. *Estuarine, Coastal and Shelf Science*, *89*(2), 163–174. https://doi.org/10.1016/j.ecss.2010.06.011

Nitsche, F. O., Ryan, W. B. F., Carbotte, S. M., Bell, R. E., Slagle, A., Bertinado, C., et al. (2007). Regional patterns and local variations of sediment distribution in the Hudson River estuary. *Estuarine, Coastal and Shelf Science*, *71*(1-2), 259–277. https://doi.org/10.1016/j.ecss.2006.07.021

Postma, H. (1961). Transport and accumulation of suspended matter in the Dutch Wadden Sea. *Netherlands Journal of Sea Research*, *1*(1-2), 148–190. https://doi.org/10.1016/0077-7579(61)90004-7

Ralston, D. K., Geyer, W. R., & Warner, J. C. (2012). Bathymetric controls on sediment transport in the Hudson River estuary: Lateral asymmetry and frontal trapping. *Journal of Geophysical Research*, *117*, C10013. https://doi.org/10.1029/2012JC008124

Ralston, D. K., & Geyer, W. R. (2009). Episodic and long-term sediment transport capacity in the Hudson River estuary. *Estuaries and Coasts*, *32*(6), 1130–1151. https://doi.org/10.1007/s12237-009-9206-4

Ralston, D. K., & Geyer, W. R. (2017). Sediment transport time scales and trapping efficiency in a tidal river. *Journal of Geophysical Research: Earth Surface*, *122*, 2042–2063. https://doi.org/10.1002/2017JF004337

Ralston, D. K., Geyer, W. R., & Lerczak, J. A. (2008). Subtidal salinity and velocity in the Hudson River estuary: Observations and modeling. *Journal of Physical Oceanography*, *38*(4), 753–770. https://doi.org/10.1175/2007JPO3808.1

Ralston, D. K., Talke, S., Geyer, W. R., Al-Zubaidi, H. A., & Sommerfield, C. K. (2019). Bigger tides, less flooding: Effects of dredging on barotropic dynamics in a highly modified estuary. *Journal of Geophysical Research: Oceans*, *124*, 196–211. https://doi.org/10.1029/2018JC014313

Ralston, D. K., Warner, J. C., Geyer, W. R., & Wall, G. R. (2013). Sediment transport due to extreme events: The Hudson River estuary after tropical storms Irene and Lee. *Geophysical Research Letters*, *40*, 5451–5455. https://doi.org/10.1002/2013GL057906

Ralston, D. K., Yellen, B., & Woodruff, J. D. (2020). *Watershed sediment supply and potential impacts of dam removals for an estuary*. https://doi.org/10.1002/essoar.10502519.1.ESSOAr

Renshaw, C. E., Magilligan, F. J., Doyle, H. G., Dethier, E. N., & Kantack, K. M. (2019). Rapid response of New England (USA) rivers to shifting boundary conditions: Processes, time frames, and pathways to post-flood channel equilibrium. *Geology*, *47*. GeoScienceWorld, 997–1000. https://doi.org/10.1130/G46702.1

Schoellhamer, D. H. (2011). Sudden clearing of estuarine waters upon crossing the threshold from transport to supply regulation of sediment transport as an erodible sediment pool is depleted: San Francisco Bay, 1999. *Estuaries and Coasts*, *34*(5), 885–899. https://doi.org/10.1007/s12237-011-9382-x

Schoellhamer, D. H., Wright, S. A., & Drexler, J. Z. (2013). Adjustment of the San Francisco estuary and watershed to decreasing sediment supply in the 20th century. *Marine Geology*, *345*, 63–71. https://doi.org/10.1016/j.margeo.2013.04.007

Sommerfield, C. K., Duval, D. I., & Chant, R. J. (2017). Estuarine sedimentary response to Atlantic tropical cyclones. *Marine Geology*, *391*, 65–75. https://doi.org/10.1016/j.margeo.2017.07.015

Syvitski, J. P., Morehead, M. D., Bahr, D. B., & Mulder, T. (2000). Estimating fluvial sediment transport: The rating parameters. *Water Resources Research*, *36*(9), 2747–2760. https://doi.org/10.1029/2000WR900133

Traykovski, P., Geyer, R., & Sommerfield, C. (2004). Rapid sediment deposition and fine-scale strata formation in the Hudson estuary. *Journal of Geophysical Research*, *109*(F2), F02004. https://doi.org/10.1029/2003JF000096

Wall, G., Nystrom, E., & Litten, S. (2008). Suspended sediment transport in the freshwater reach of the Hudson River estuary in eastern New York. *Estuaries and Coasts*, *31*(3), 542–553. https://doi.org/10.1007/s12237-008-9050-y

Walling, D. E. (1977). Assessing the accuracy of suspended sediment rating curves for a small basin. *Water Resources Research*, *13*(3), 531–538. https://doi.org/10.1029/WR013i003p00531

Walling, D. E., Owens, P. N., & Leeks, G. J. L. (1998). The role of channel and floodplain storage in the suspended sediment budget of the river Ouse, Yorkshire, UK. *Geomorphology*, *22*, 225–242. https://doi.org/10.1016/S0169-555X(97)00086-X

Warrick, J. A., Madej, M. A., Goñi, M. A., & Wheatcroft, R. A. (2013). Trends in the suspended-sediment yields of coastal rivers of northern California, 1955–2010. *Journal of Hydrology*, *489*, 108–123. https://doi.org/10.1016/j.jhydrol.2013.02.041

Warrick, J. A., & Rubin, D. M. (2007). Suspended-sediment rating curve response to urbanization and wildfire, Santa Ana River, California. *Journal of Geophysical Research 112*: F02018.

Wellershaus, S. (1981). Turbidity maximum and mud shoaling in the Weser estuary. *Archiv für Hydrobiologie*, *92*(2), 161–198.

Woodruff, J. D., Geyer, W. R., Sommerfield, C. K., & Driscoll, N. W. (2001). Seasonal variation of sediment deposition in the Hudson River estuary. *Marine Geology*, *179*, 105–119. https://doi.org/10.1016/S0025-3227(01)00182-7

Yellen, B., Woodruff, J. D., Cook, T. L., & Newton, R. M. (2016). Historically unprecedented erosion from tropical storm Irene due to high antecedent precipitation. *Earth Surface Processes and Landforms*, *41*, 677–684. https://doi.org/10.1002/esp.3896

Yellen, B., Woodruff, J. D., Kratz, L. N., Mabee, S. B., Morrison, J., & Martini, A. M. (2014). Source, conveyance and fate of suspended sediments following Hurricane Irene. New England, USA. *Geomorphology*, *226*, 124–134. https://doi.org/10.1016/j.geomorph.2014.07.028

Yellen, B., Woodruff, J. D., Ladlow, C., Ralston, D. K., Fernald, S., & Lau, W. (2020). Rapid tidal marsh development in anthropogenic backwaters. *EarthArXiv*. https://doi.org/10.31223/osf.io/ga5pm